Chapter 5

Photoelectric Effect

By R. J. MAURER, University of Illinois

1. General Considerations [1]†

The photoelectric effect was discovered by Hertz and Hallwachs in 1887–1888. The effect consists of the ejection of electrons from the surface of a solid when electromagnetic radiation is incident upon it. Although the photoelectric effect occurs at the surfaces of semiconductors and insulators, metallic surfaces have been the chief object of investigation.

The number of photoelectrons produced per unit time is proportional to the intensity of the incident electromagnetic radiation; so the photoelectric yield, which is the number of photoelectrons per incident quantum of radiation, is independent of intensity. The most important factors which determine the photoelectric yield are the nature of the metal, the state of contamination of its surface by adsorbed gas, and the frequency of the radiation. The state of polarization and the angle of incidence of the radiation may also be of considerable importance in particular if the surface exhibits specular reflection. Because of the difficulty in preparing gas-free surfaces there are almost no photoelectric data available which can be considered characteristic of clean metal surfaces.

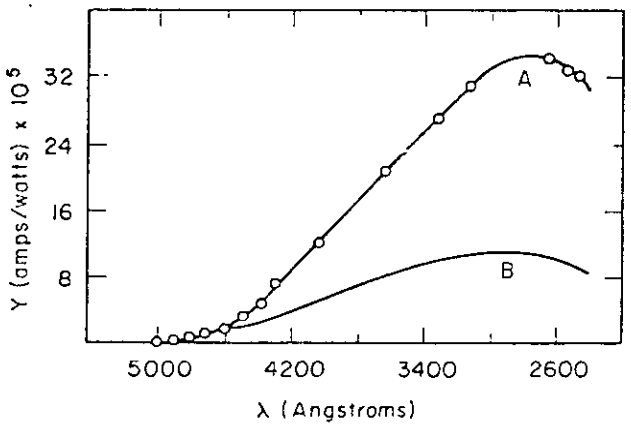

FIG. 5.1. The spectral distribution curve of barium. (*A*) Experimental; (*B*) theoretical. [*R. J. Maurer: Phys. Rev.*, **57**: 653 (1940).]

The typical dependence of the photoelectric yield on frequency is shown in Fig. 5.1 for a barium surface [2]. A characteristic feature of the spectral distribution curve is an apparent threshold frequency, a minimum frequency of radiation for which photoelectric emission is detectable. Since the photoelectric yield decreases rapidly as the frequency of the incident radiation is decreased but does not become zero, the apparent threshold frequency depends upon the sensitivity of the experimental apparatus. The apparent threshold also depends upon the temperature of the surface since the photoelectric yield increases with increasing temperature for frequencies near the apparent threshold. The photoelectric yield usually exhibits a maximum at a frequency somewhat less than twice the apparent threshold frequency. Because the apparent threshold for the majority of the metals lies in the vicinity of 4 ev, the maximum of the spectral distribution curve ordinarily occurs in a relatively inaccessible region of the ultraviolet. Of the pure metals, the alkalis and some of the alkaline earths possess apparent thresholds at sufficiently small frequencies to permit the maximum of the spectral distribution curve to be conveniently observed.

The photoelectric yield of pure metal surfaces at the maximum of the spectral distribution curve is of the order of 10^{-3} electrons per incident quantum. A few solids exhibit much larger yields. Caesium-antimony is an outstanding example with a maximum yield of approximately 10^{-1} electrons per incident quantum.

Specular surfaces usually exhibit a maximum yield for an angle of incidence of the radiation near 60°. The yield may be larger by a factor as much as 10 for radiation polarized with the electric vector in the plane of incidence than when the electric vector is perpendicular to the plane of incidence and therefore parallel to the surface.

The kinetic energies of the individual photoelectrons which are ejected by a fixed frequency and intensity of radiation are distributed over a range from zero to indefinitely large values. The form of the energy distribution function, $n(\epsilon)$, the relative number of electrons of energy ϵ per unit energy range, is shown in Fig. 5.2. The relative number of fast electrons is

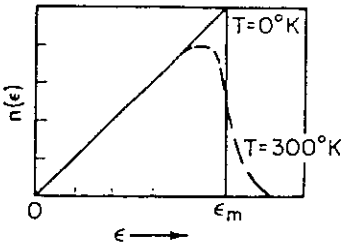

FIG. 5.2. The theoretical distribution in energy of photoelectrons from a metal, according to DuBridge.

† Numbers in brackets refer to References at end of chapter.

small and the original investigators concluded that a maximum kinetic energy of emission, ϵ_M, existed. As in the case of the photoelectric threshold, the apparent maximum emission energy is due to the finite sensitivity of experimental apparatus and the extremely rapid decrease in the number of fast electrons with increasing energy. A prime achievement of modern photoelectric research has been to give a definite and physical interpretation to the concepts of "threshold frequency" and "maximum kinetic energy of emission."

The original experiments on the distribution in energy of photoelectrons showed that the apparent maximum kinetic energy of emission was independent of the intensity but was a function of the frequency of the radiation. These results led Einstein to the hypothesis that photoelectric emission was a quantum effect in which the energy, $h\nu$, of a quantum of radiant energy was "absorbed" by an electron in the metal which thereby increased its kinetic energy by this amount. The observed distribution in energy of the photoelectrons was assumed to result from energy losses suffered by the electrons in escaping from the metal. Einstein suggested that the maximum kinetic energy of emission is given by

$$\epsilon_M = h\nu - \phi \tag{5.1}$$

where ϕ, the work function of the metal surface, is the minimum possible loss of kinetic energy by the escaping photoelectron. Despite the difficulties inherent in the concept of a maximum kinetic energy of emission, Millikan's experimental confirmation of this equation in 1916 offered powerful support to the quantum theory of radiation and provided an independent value of Planck's constant, h. It is to be noted that Eq. (5.1) implies a photoelectric threshold frequency $\nu_0 = \phi/h$ for $\epsilon_M = 0$. Further support for the quantum theory of the photoelectric effect was given by the experiments of Lawrence and Beams, who showed that the time lag between the incidence of radiation on a surface and the appearance of photoelectrons is less than 10^{-9} sec.

2. The Spectral Distribution Function

Within the framework of a general theory of the interaction of electromagnetic radiation with a solid, photoelectric emission appears as a by-product of the process of optical absorption. The theory of photoelectric emission begins with an assumed model of the solid which specifies the allowed states of the electrons in terms of their wave functions and energy levels; proceeds with a calculation of the optical transition probabilities connecting the initial and excited states of the electrons; and concludes with a calculation of the probability of an excited electron escaping through the surface. An excited electron which possesses sufficient kinetic energy to cross the potential energy barrier that exists at the surface of a solid may be reflected back into the solid by the barrier. In the case of a typical metal, although the radiation penetrates to a depth of approximately 10^{-5} cm below the surface, the photoelectrons come from a much thinner surface layer because electron-electron collisions limit the mean free path of an excited electron to a distance of the order of 10^{-7} cm [3]. In an insulator, electron-phonon collisions may limit the volume from which emission can be obtained.

In the Bloch approximation the allowed optical transitions of an electron moving in the periodic potential of a crystal are restricted to transitions between states of the same reduced wave number in different bands. This selection rule is illustrated in Fig. 5.3 for a one-dimensional metal by the vertical

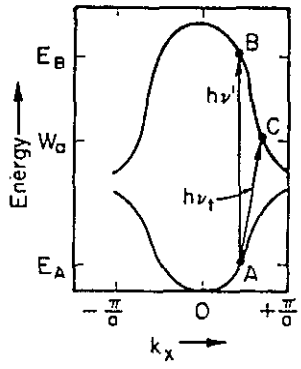

FIG. 5.3. Energy versus reduced wave-number vector for a one-dimensional metal with lattice constant a.

arrow connecting states A and B. If A represents a state lying at the surface of the Fermi distribution of electrons in a conduction band, then $E_B - E_A = h\nu'$ defines the threshold frequency for volume optical absorption by the conduction electrons. If W_a represents the height of the surface potential energy barrier, the energy difference, $W_a - E_A$, is the thermionic work function of the metal. In all cases where precise and comparable measurements have been made it has been found that the thermionic work function and the photoelectric work function, $h\nu_t$, of metals agree closely. It appears that optical transitions occurring between states such as A and C are the important ones for photoelectric emission near the threshold [4].

At the surface of a metal, the potential is not periodic and the optical transitions of an electron moving in the field of the surface potential energy barrier are not restricted by the volume optical selection rules. The observed photoelectric effect results from a *surface* optical absorption which is ignored as negligible in the conventional theory of the optical properties of metals [5]. Photoelectric measurements on the high-work-function metals, such as tungsten, have probably not been extended to sufficiently large frequencies to observe volume emission, while the alkali metals with their small work functions are optically transparent, the volume absorption being too small to contribute a detectable component to the observed surface emission.

The theory of surface photoelectric emission has been developed with the use of the Sommerfeld model of a metal (Fig. 5.4) which automatically excludes the possibility of volume absorption since the optical transition probabilities of an electron in a constant potential vanish [6]. At the surface of the metal, one may assume a discontinuous rise in potential energy of amount W_a or, more plausibly, a rapid but smoothly increasing potential energy which becomes the image

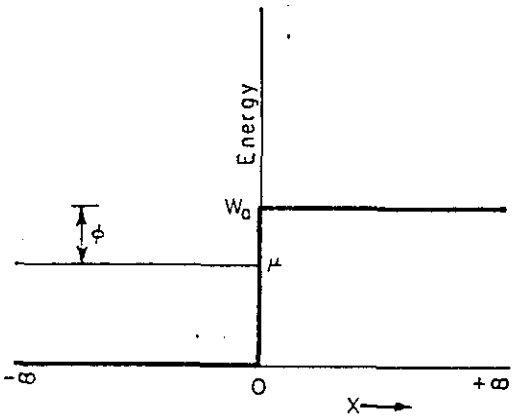

FIG. 5.4. The Sommerfeld model of a metal with a discontinuous potential step of magnitude W_a at the surface. The Fermi energy is μ and the work function is φ.

potential, $V = -(e^2/4x)$, at a distance of the order of 10^{-7} cm from the surface.

Inside the metal, the density of states, $D(E)$, is given by

$$D(E) = \frac{1}{2\pi^2}\left(\frac{2m}{\hbar^2}\right)^{3/2} E^{1/2} \tag{5.2}$$

where the zero of energy has been taken as the constant potential energy of an electron inside the metal. The population of the states by electrons is determined by the Fermi function

$$f(E) = \frac{1}{e^{E-\mu/kT} + 1} \tag{5.3}$$

where μ, the energy of the Fermi level, represents the kinetic energy of the most energetic electron in the metal at the absolute zero of temperature. Because of spin each state may be occupied by two electrons. The position of the Fermi level at 0°K can be calculated if the density of free electrons, n, is known.

$$\mu = \frac{h^2}{2m}\left(\frac{3}{8\pi}n\right)^{2/3} \tag{5.4}$$

The small temperature dependence of the Fermi energy may be neglected.

If the metal is assumed to extend indefinitely in the y, z and negative x directions with the surface at the plane $x = 0$, the initial unperturbed wave functions of the electrons are

$$\begin{aligned}\psi_k &= \alpha_k[\exp(-ik_x x) + a_k \exp(ik_x x)] \\ &\qquad \exp(ik_y y + ik_z z) \qquad x < 0 \\ \psi_k &= \alpha_k b_k \exp(-px)\exp(ik_y y + ik_z z) \quad x > 0\end{aligned} \tag{5.5}$$

where $b_k = 1 + a_k$, $pb_k = ik_x(1 - a_k)$, and p is a real constant. The wave-number vector $\mathbf{k}$ of an electron in the metal is related to its kinetic energy by the relation

$$k^2 = k_x^2 + k_y^2 + k_z^2 = \frac{8\pi^2 m}{h^2} E \tag{5.6}$$

The effect of the incident radiation upon the system can be calculated by first-order perturbation theory. The character of the radiation is defined by the form assigned to its vector potential $\mathbf{A}$, which appears as the perturbation in the Hamiltonian of the Schroedinger equation

$$-\frac{ihe}{2\pi mc}(\mathbf{A}, \operatorname{grad} u) \tag{5.7}$$

Here u is the perturbed wave function of an electron. A plausible procedure for fixing the form of the vector potential inside and outside the metal is to use Maxwell's equations and the experimentally determined optical constants of the metal. A still simpler procedure is to ignore the optical constants and use the vector potential of a plane wave

$$\mathbf{A} = \mathbf{A}_0 \cos 2\pi\nu\left(t + \frac{x\cos\theta + y\sin\theta}{c}\right) \tag{5.8}$$

where θ is the angle of incidence. Reflection, refraction, and absorption are ignored by this simpler procedure so that the *absolute* yield obtained in this manner is not accurate.

Having obtained the perturbed wave functions for the region $x > 0$, the current density per electron, j_x, is calculated

$$j_x = \frac{eh}{4\pi mi}\left(u\frac{\partial u^*}{\partial x} - u^*\frac{\partial u}{\partial x}\right) \tag{5.9}$$

and summed over all initial states which after absorption of a quantum, $h\nu$, can contribute to the current. If this total photoelectric current density is divided by the rate at which quanta of radiation energy are incident upon the surface, the photoelectric yield results.

The theoretical spectral distribution curve for barium, which is shown in Fig. 5.1, was calculated by this procedure. A discontinuous rise in potential was assumed at the surface of the metal. The magnitude of the potential jump W_a was fixed by addition of the observed work function, 2.48 ev, to the calculated Fermi energy. It was assumed that barium contained 1.8 free electrons per atom. The simplest form for the vector potential, Eq. (5.8), was taken. The absolute yield as shown in Fig. 5.1 was fixed by a procedure which is described later.

The yield is given by the following integral, the integrand of which is made up of three easily interpretable terms.

$$\begin{aligned}Y_x = \frac{e^3\nu_a \sin^2\theta}{4\pi^2 m^2 c\cos\theta} &\iiint\left(\frac{2}{8\pi^3}\right)\frac{dk_x\,dk_y\,dk_z}{1+\exp(E-\mu)/kT}\cdot \\ &\frac{1}{\nu^4}\frac{k_x^2}{(k_x^2+\tilde{\mu}\nu)^{1/2}}\cdot \\ &\frac{4(k_x^2+\tilde{\mu}\nu)^{1/2}[k_x^2+\tilde{\mu}(\nu-\nu_a)]^{1/2}}{\{(k_x^2+\tilde{\mu}\nu)^{1/2}+[k_x^2+\tilde{\mu}(\nu-\nu_a)]^{1/2}\}^2}\end{aligned} \tag{5.10}$$

where $W_a = h\nu_a$, $\tilde{\mu} = 8\pi^2 m/h$, $E = hk^2/\tilde{\mu}$, and μ is the Fermi energy. The integration is extended over all electrons in the metal whose wave-number vectors, k_x, normal to the surface are sufficient to enable them to escape after absorption of a quantum.

The first term in the integrand is the Fermi function; the exponential factor in it can be neglected at room temperature for $(\mu - E)$ greater than a few

hundredths of an electron volt; the limits of integration being fixed in this case by taking μ as the energy of the most energetic electron in the metal. This is equivalent to treating the electron gas as if it were at 0°K. The temperature is therefore unimportant except very near the apparent threshold frequency.

The third term in the integrand is the transmission coefficient of a discontinuous potential step. For a simple continuous step, such as the image potential barrier, the transmission coefficient is almost unity for practically all electrons having sufficient energy to escape [7, 8]. The theory is improved, therefore, by discarding the third term of the integrand. This was done in calculating the theoretical curve of Fig. 5.1.

The second term in the integrand is a product of the probability that an electron in a state of energy E will be excited to a state of energy $E + h\nu$ and the probability that an electron, in the state of energy $E + h\nu$, will escape through the surface.

Only the component of the vector potential parallel to the plane of incidence gives rise to photoelectrons with the ideally plane surface which has been assumed. For this reason, the yield is zero for normal incidence of the radiation.

Mitchell has calculated absolute yields for the case of an image potential barrier and a rough surface which is composed of elements small compared to the wavelength of the radiation but large compared to the electron wavelength [6]. In addition, he has included the variation of the optical constants with wavelength for the case of sodium. With these assumptions the effect of the state of polarization and the angle of incidence of the radiation can be observed. The theory is only moderately successful in reproducing the experimentally observed spectral distribution curves. The calculated frequency dependence of the yield is not in very good agreement with experiment in the case of sodium and the absolute magnitude of the yield is too small by a factor of about 50 for both sodium and barium [2]. The extent to which the experimental data can be considered representative of the behavior of clean metal surfaces is, of course, always open to question.

Schiff and Thomas have given a quantum theory of reflection and refraction at a metallic surface and shown that the component of the electric vector which is perpendicular to the surface oscillates with large amplitude near the surface [9]. It must be concluded that the use of classical optical theory in photoelectric theory is of dubious validity. Makinson has given, however, a semiclassical treatment of photoelectric emission from a totally reflecting metal which approximates the procedure of Schiff and Thomas and compared his results with data from potassium [10]. The agreement is not very good and the results serve to emphasize the difficulties faced in attempting a realistic theory of the spectral distribution curve.

If the theory of the spectral distribution curve is restricted to a calculation of the relative yield for a narrow range of frequencies near the apparent threshold, Mitchell's equation (5.10) can be subjected to a number of approximations. As before, the transmission coefficient of the barrier can be omitted. The frequency dependence of the second term of the integrand can be ignored and this term taken proportional to k_x. The relative yield is then

$$Y(\nu,T) = \iiint \frac{k_x\, dk_x\, dk_y\, dk_z}{1 + \exp\,(E - \mu)/kT} \qquad (5.11)$$

The range of integration is over all initial states of energy E which after absorption of a quantum possess sufficient kinetic energy associated with the component of the propagation vector k_x, normal to the surface, to escape. These are states for which k_x is greater than $[(8\pi^2 m/h^2)(W_a - h\nu)]^{1/2}$. The relative yield of Eq. (5.11) is proportional to the number of electrons which strike unit area of surface per unit time and escape. In this approximation, the problem of photoemission is reduced to that of thermionic emission from a Sommerfeld metal with a nonreflecting barrier of magnitude $W_a - h\nu$ instead of W_a.

The theory, in this form, is DuBridge's modification of Fowler's theory which was published before Mitchell attempted a complete theory of the spectral distribution curve [11, 12]. The Fowler-DuBridge theory is extremely useful because it quantitatively accounts for the temperature dependence of the yield near the apparent threshold and provides an unambiguous and physically meaningful definition of a photoelectric threshold frequency. The yield Y, as given by Eq. (5.11), can be expressed as

$$Y = \alpha A T^2 \phi(x) \qquad (5.12)$$

where $\phi(x)$ is the series

$$\phi(x) = \left[e^x - \frac{e^{2x}}{2^2} + \frac{e^{3x}}{3^2} - \cdots \right] \qquad x \leq 0 \qquad (5.13)$$

$$\phi(x) = \left[\frac{x^2}{2} + \frac{\pi^2}{6} - \left(e^{-x} - \frac{e^{-2x}}{2^2} + \frac{e^{-3x}}{3^2} - \cdots \right) \right] \qquad x \geq 0$$

The parameter x is

$$x = \frac{h\nu - (W_a - \mu)}{kT} \qquad (5.14)$$

and Fowler *defined* the photoelectric threshold frequency, ν_0, by

$$h\nu_0 = W_a - \mu \qquad (5.15)$$

so that $h\nu_0$ is, by definition, equal to the thermionic work function. The constant $A = 4\pi mk^2/h^3$ and is closely related to the universal constant of thermionic emission theory. The theoretically undetermined constant α is the fraction of electrons that arrive at unit area of the surface in unit time, absorb a quantum, and escape, when the incident radiation intensity is unity.

Extensive measurements by DuBridge, his coworkers, and others have amply verified that the above theory gives an adequate account of the temperature and frequency dependence of the relative yield near the threshold [12]. Theory and experiment are conveniently compared by using Eq. (5.12) in the form

$$\log \frac{Y}{T^2} = \log\,(\alpha A) + \log\,\phi(x) \qquad (5.16)$$

and plotting $\log\,(Y/T^2)$ vs. x. Since $\log\,(Y/T^2)$ is a universal function of x, if the experimental data are

$$n(\epsilon)\,d\epsilon = v_x \left\{1 - \left[\frac{W_a - h\nu}{\epsilon + (W_a - h\nu)}\right]^{1/2}\right\} \frac{(\epsilon + W_a - h\nu)^{1/2}\,d\epsilon}{\exp\left[(\epsilon - \epsilon_M)/kT\right] + 1} \quad (5.20)$$

The term $\{1 - [(W_a - h\nu)/(\epsilon + (W_a - h\nu))]^{1/2}\}$ is the probability that an electron of energy E inside the metal has its velocity vector directed so that the normal kinetic energy, $\frac{1}{2}mv_x^2$, is greater than or equal to $W_a - h\nu$. If $\frac{1}{2}mv_x^2$ is set equal to $W_a - h\nu$, an approximate form of Eq. (5.20) is obtained

$$n(\epsilon)\,d\epsilon = \frac{\epsilon\,d\epsilon}{\exp\left[(\epsilon - \epsilon_M)/kT\right] + 1} \quad (5.21)$$

where $$\epsilon_M = h\nu - (W_a - \mu) = h\nu - \varphi \quad (5.22)$$

The energy ϵ_M is the maximum kinetic energy of emission of photoelectrons from a surface at 0°K. At higher temperatures, a maximum kinetic energy of emission does not exist. The energy distribution, according to DuBridge's equation (5.21), is shown in Fig. 5.2.

The distribution in energy of photoelectrons is usually investigated by observing the photocurrent as a function of applied potential in a spherical photocell, as illustrated in Fig. 5.6. The small photo-

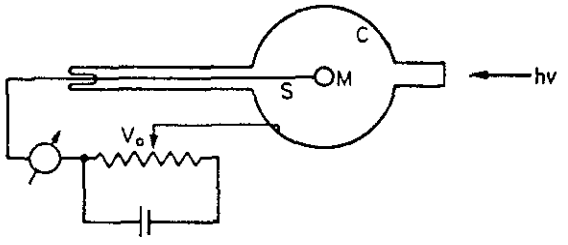

FIG. 5.6. Photocell for energy distribution measurements. M, emitter; S, support; C, collector; V_a, applied potential.

sensitive surface M is placed at the center of the spherical collector C, which is ordinarily a film of graphite or metal on the inner surface of the glass envelope. With this geometry, the velocity vectors of the photoelectrons are radially directed along the lines of force of the electric field between emitter and collector. Only the photoelectrons with kinetic energy $\epsilon > eV$ reach the collector C when the retarding potential difference V_a is applied between emitter and collector. Because of the contact difference of potential, $V_c = -(\varphi_c - \varphi_M)/e$, the potential difference between points just outside the surfaces of M and C is $V = V_a + V_c$.

According to DuBridge's theory the current-voltage curve $i(V_a)$ is given by the integral

$$i(V_a) = \int_{-e(V_a+V_c)}^{\infty} \frac{\epsilon\,d\epsilon}{\exp\left[(\epsilon - \epsilon_M)/kT\right] + 1} \quad (5.23)$$

The form of the current-voltage curve is shown in Fig. 5.7. For a surface at the absolute zero of temperature the exponential can be neglected and the upper limit of integration replaced by ϵ_M. The current-voltage curve is then a parabola. The observed photocurrent is zero for a retarding potential V_0 such that $-e(V_0 + V_c) = \epsilon_M$ or $V_0 = -(h\nu - \varphi_c)/e$ since $\epsilon_M = h\nu - \varphi_M$. φ_c is the work function of the collector. The current rises to a saturation value i_s

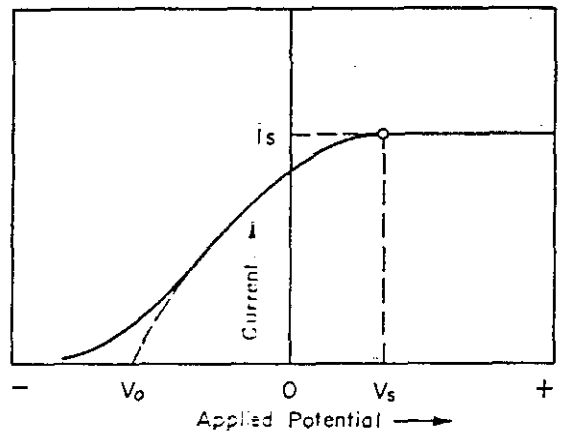

FIG. 5.7. Theoretical current-voltage curve according to DuBridge's theory. i_s, saturation photocurrent; V_s, saturation potential; V_0, stopping potential at 0°K.

for an applied potential $V_s = -V_c$. If V_s and V_0 are determined from the observed current-voltage curve, the work function of the emitter surface can be obtained

$$\varphi_M = h\nu - e(V_s - V_0) \quad (5.24)$$

For temperatures other than 0°K, the photocurrent decreases asymptotically to zero as the retarding potential is increased. The integral of Eq. (5.23) can be evaluated in terms of the series

$$i = \alpha A T^2 \left(\frac{\pi^2}{6} - \frac{1}{2}(x^2 - x_M^2) + x \ln\left[1 + \exp(x - x_M)\right] - \left\{\exp(x - x_M) - \frac{\exp\left[2(x - x_M)\right]}{2^2} + \frac{\exp\left[3(x - x_M)\right]}{3^2} - \cdots\right\}\right) \quad \text{for } x \le x_M \quad (5.25)$$

$$i = \alpha A T^2 \left(x(x_M - x) + x \ln\left[1 + \exp(x - x_M)\right] + \left\{\exp\left[-(x - x_M)\right] - \frac{\exp\left[-2(x - x_M)\right]}{2^2} + \cdots\right\}\right) \quad \text{for } x \ge x_M$$

Here $x = \epsilon/kT$ and $x_M = \epsilon_M/kT$. For $x_M > 10$ and $x > x_M$, Eq. (5.25) may be approximated by

$$\log \frac{i}{xT^2} = \log(\alpha A) + \chi(x - x_M) \quad (5.26)$$

where $\chi(x - x_M)$ is the universal function of $(x - x_M)$

$$\chi(x - x_M) = \log\left\{\exp\left[-(x - x_M)\right] - \left(\tfrac{1}{4}\right)\exp\left[-2(x - x_M)\right]\right\} \quad (5.27)$$

The experimental current-voltage curve can be plotted as $\log(i/xT^2)$ vs. x, where $x = \epsilon/kT$ and $\epsilon = -e(V_a - V_s)$. The shift parallel to the x axis necessary to bring the experimental curve into coincidence with the theoretical curve (5.27) determines x_M and ϵ_M. After ϵ_M is found in this manner, V_0 can be obtained from $\epsilon_M = -e(V_0 - V_s)$. In this manner, V_0 can be determined from current-voltage data obtained at any temperature. DuBridge and

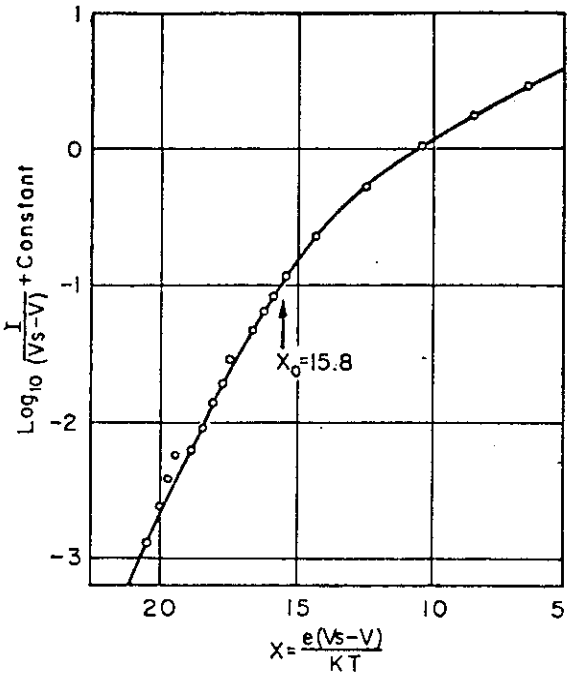

FIG. 5.8. The current-voltage curve of polycrystalline tungsten. The solid curve is DuBridge's theory. T = 300°K; $h\nu$ = 4.89 ev; $x_0 = (h\nu - \varphi)/kT$;

$$V_0 = +0.21 \text{ volts}$$

V_s = +0.62 volts. [*L. Apker, E. Taft, and J. Dickey: Phys. Rev.*, **73**: 46 (1948).]

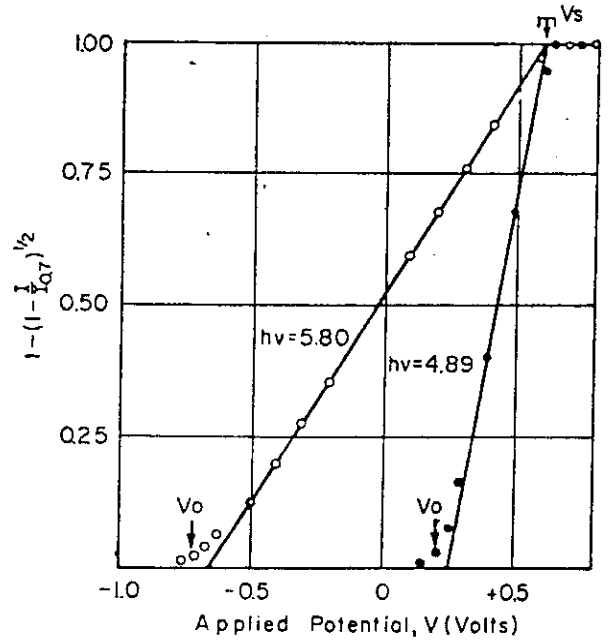

FIG. 5.9. Current-voltage curves of polycrystalline tungsten. T = 300°K; $h\nu$ = 4.89 ev and 5.80 ev; V_s = +0.62 volts. [*L. Apker, E. Taft, and J. Dickey: Phys. Rev.*, **73**: 46 (1948).]

his coworkers have shown that the high-energy tails of experimental current-voltage curves are in excellent agreement with this theory [12]. Figure 5.8 shows a comparison of theory with data obtained from polycrystalline tungsten by Apker, Taft, and Dickey [16]. Figure 5.9 shows complete current-voltage curves for this surface. As predicted by DuBridge's theory, the current-voltage curve is parabolic except for the high-energy tail. The work function of this surface was determined as 4.48 ± 0.03 ev from the analysis of the energy distribution data. Spectral distribution curves and isochromatic curves analyzed by the Fowler-DuBridge procedure yielded identical work functions of 4.49 ± 0.02 ev.

Mitchell has extended his treatment of the surface photoelectric effect at an image potential barrier to include the energy distribution of the photoelectrons [6]. For electron energies near ϵ_M, his energy distribution function is the same as DuBridge's. Mitchell's theory predicts relatively fewer slow electrons than DuBridge's theory because the probability of absorption of a quantum depends upon the initial state of the electron.

Experimental energy distributions usually have for small energies the general form predicted by Mitchell's theory. Apker has shown, however, that energy distributions are, in general, untrustworthy at small energies because of distortion of the electric field in the photocells as a result of contact differences between the emitter and its support. Extreme care was exercised to remove this difficulty in obtaining the data shown in Figs. 5.8 and 5.9.

Berglund and Spicer [17, 18] have investigated photoemission from copper and silver excited by photons of energy considerably greater than the threshold energy. The band structure of the metal is of primary importance for this volume emission. Figure 5.10 shows the energy distribution of photo-

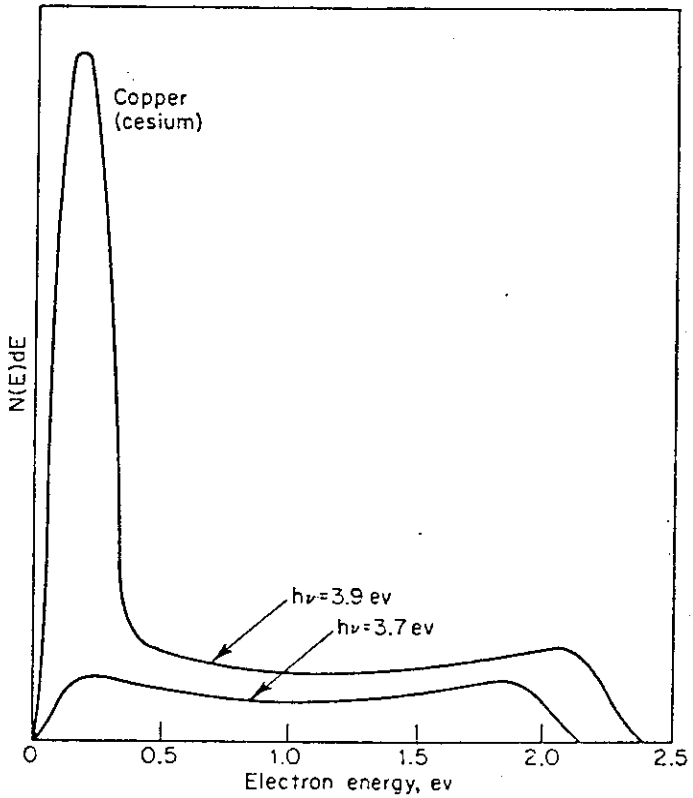

FIG. 5.10. Energy distribution of photoemitted electrons from copper. [*C. N. Berglund and W. E. Spicer: Phys. Rev.*, **136**: A1044 (1964).]

emitted electrons from a copper surface whose threshold has been reduced to 1.55 ev by a surface layer of cesium. The large, low-energy peak in the energy distribution that is observed with exciting radiation of photon energy $h\nu$ = 3.9 ev is attributed to exci-

tation of electrons from the d band lying 2 ev below the Fermi level. The energy-distribution curve obtained with 3.7-ev photons shows only a trace of slow electrons excited from the d band. The photoemission is due to indirect optical transitions of the type illustrated by the arrow AC of Fig. 5.3. Direct transitions were observed for photon energies greater than 4.5 ev, but indirect transitions dominated the excitation process. The reason for this breakdown of the selection rules of the Bloch approximation is not understood [19].

Electron-electron scattering is of major importance in copper for photon energies greater than 6 ev, producing a large, low-energy peak in the energy distribution of the photoelectrons at about 0.5 ev. A low-energy peak in the energy distribution of the photoelectrons from silver, which appears for photon energies greater than 4 ev, can be attributed to a contribution to the photoemission from the Auger effect. For both silver and copper it was possible to deduce the density of states and the location of important symmetry points of the energy bands from the photoelectric data.

4. Semiconductors and Insulators

The distribution in energy of electrons in semiconductors and insulators is so different from that in metals that, for this reason alone, quite different photoelectric behavior is expected [20, 21]. Figure 5.11 compares the energy-level scheme for a typical

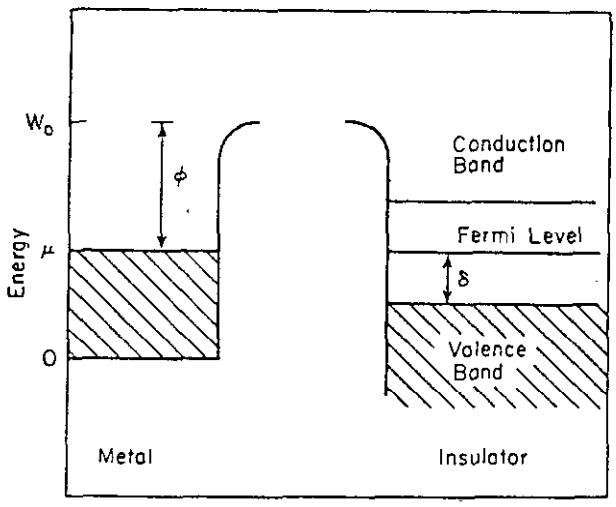

FIG. 5.11. The electronic energy levels of metals and insulators.

insulator and a metal of the same work function, $\varphi = W_a - \mu$. The Fermi level μ of the insulator lies within the forbidden energy region and approximately midway between the most energetic level of the filled valence band and the lowest level of the empty conduction band. The energy levels in the vicinity of the Fermi level μ in the case of a metal are filled with electrons and furnish the most energetic photoelectrons. In the insulator the electrons of largest energy have an energy δ less than μ. The distribution in energy of photoelectrons from an insulator may be expected to contain few fast electrons as compared with that of a metal of the same thermionic work function. The temperature dependence of the energy distribution will also be quite unlike that of a metal.

Figure 5.12 shows current-voltage curves for amorphous arsenic compared with a metal of the same

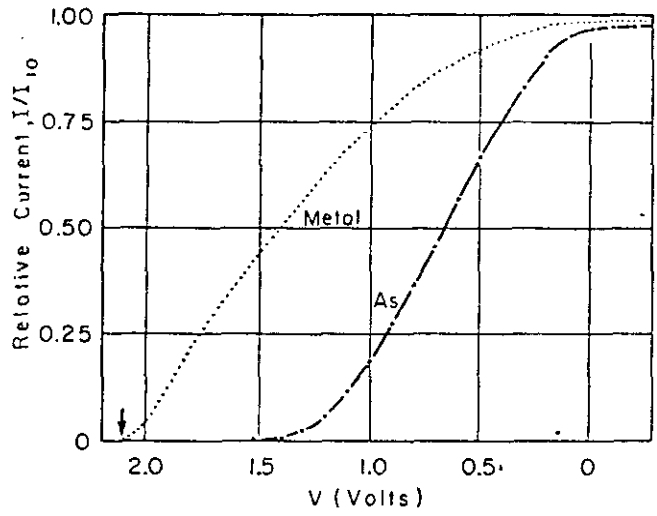

FIG. 5.12. The current-voltage curve of amorphous arsenic and of a metal with the same work function, 4.66 ev. $T = 300°K$; $h\nu = 6.71$ ev. The arrow marks V_0, the stopping potential for 0°K. [*E. Taft and L. Apker: Phys. Rev.*, **75**: 1181 (1949).]

work function $\varphi = 4.66$ ev, which satisfies DuBridge's theory [22]. As expected, the arsenic energy distribution contains few fast electrons and the current becomes unmeasurable at a retarding potential of -1.5 volts. The stopping potential, V_0, for a metal of the same work function was -2.05 ev in this experiment. The top of the valence band in arsenic appears to lie below the Fermi level by an amount $\delta = 0.5$ ev. Similar behavior is observed with tellurium, germanium, and boron surfaces [23]. There is evidence, however, that filled surface states which lie between the Fermi level and the top of the valence band may contribute some photoemission of fast electrons.

The absence of filled energy levels in the gap δ between the Fermi level and the top of the filled valence band affects the form of the spectral distribution curve. The photoelectric threshold energy $h\nu_0$ of an insulator or semiconductor is not equal to the thermionic work function $(W_a - \mu)$ but is given by $(W_a - \mu + \delta)$. Figure 5.13 shows spectral distribution curves of tellurium, germanium, and platinum surfaces of the same work function, $\varphi = 4.76$ ev [23]. The decrease in photoelectric response for quantum energies less than $h\nu = W_a - \mu$ is clearly visible; the photocurrents from the tellurium surface were not measurable for $h\nu < 5.0$ ev.

The spectral distributions of the quantum yields of atomically clean surfaces of silicon, germanium, gallium arsenide and antimonide, and indium arsenide and antimonide are approximately proportional to $(h\nu - h\nu_t)^3$ near ν_t, the photoelectric threshold frequency [24]. This emission is probably due to indirect optical transitions associated with the surface. A few tenths of an electron volt above the photoelectric threshold, volume optical absorption becomes more important than the surface absorption, and,

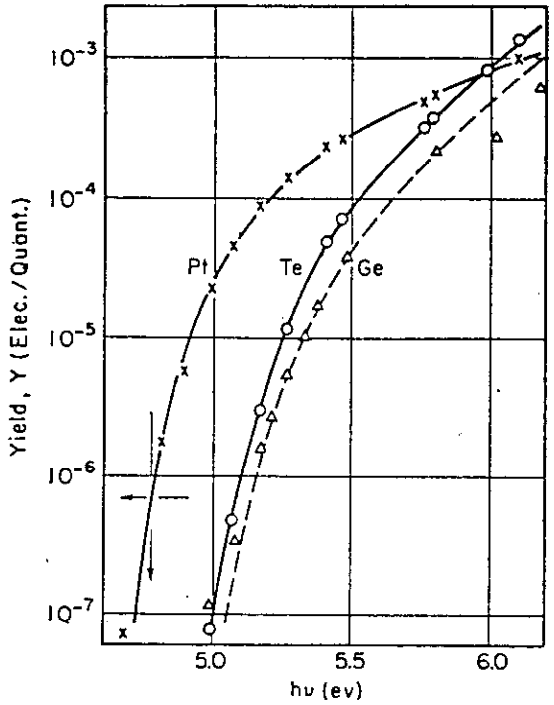

FIG. 5.13. Spectral distrubution curves of platinum, tellurium, and germanium. The solid curve through the platinum data is Fowler's theory. $T = 300°K$. The three surfaces have the same thermionic work function, 4.76 ev. [*L. Apker, E. Taft, and J. Dickey: Phys. Rev.*, **74**: 1462 (1948).]

in agreement with the theory of Kane, the yield increases linearly with $h\nu - h\nu'$, where ν' is the threshold for direct optical transitions [25, 26]. Both the spectral-distribution curves and the energy-distribution curves have yielded important information concerning energy-band structures. The band structure of lead telluride has been investigated in this manner [27]. Brust has made a detailed band-theoretical investigation of the photoelectric effect in silicon and obtained qualitative agreement with the results of Spicer [28, 29] and of Gobelli and Allen.

Allen and Gobelli [30] have compared the photoelectric thresholds and work functions of systematically doped p- and n-type silicon samples. As the Fermi level approaches the conduction or valence bands, the surface-state charge changes, with accompanying bending of the bands as they approach the surface. The resulting changes in the photoelectric threshold and work function make it possible to deduce the concentration of surface states and draw limited conclusions concerning their distribution in energy.

References

1. Hughes, A. L., and L. A. DuBridge: "Photoelectric Phenomena," McGraw-Hill, New York, 1932. Zworykin, V. K., and E. G. Ramberg: "Photoelectricity," Wiley, New York, 1949.
2. Maurer, R. J.: Photoelectric and Optical Properties of Sodium and Barium, *Phys. Rev.*, **57**: 653 (1940).
3. Sommerfeld, A., and H. Bethe: "Handbuch der Physik," Chap. 3, Springer, Berlin, 1933.
4. Fan, H. Y.: *Phys. Rev.*, **68**: 43 (1945).
5. Tamm, I., and Schubin, S.: *Z. Physik*, **68**: 97 (1931).
6. Mitchell, K.: Theory of the Surface Photoelectric Effect in Metals, *Proc. Roy. Soc.* (*London*), **A146**: 442 (1934); **A153**: 513 (1936).
7. L. Nordheim: *Proc. Roy. Soc.* (*London*), **A121**: 626 (1928).
8. A. G. Hill: Energy Distribution of Photoelectrons from Sodium, *Phys. Rev.*, **53**: 184 (1938).
9. Schiff, L., and L. Thomas: Quantum Theory of Metallic Reflection, *Phys. Rev.*, **47**: 860 (1935).
10. Makinson, R. E. B.: Metallic Reflexion and the Surface Photoelectric Effect, *Proc. Roy. Soc.* (*London*), **A162**: 367 (1937).
11. Fowler, R. H.: Analysis of Photoelectric Sensitivity Curves, *Phys. Rev.*, **38**: 45 (1931).
12. DuBridge, L. A.: "New Theories of the Photoelectric Effect," Hermann & Cie, Paris, 1935.
13. DuBridge, L. A., and W. W. Roehr: Photoelectric and Thermionic Properties of Palladium, *Phys. Rev.*, **39**: 99 (1932).
14. DuBridge, L. A.: A Test of Fowler's Theory of Photoelectric Emission, *Phys. Rev.*, **39**: 108 (1932).
15. DuBridge, L. A.: Theory of the Energy Distribution of Photoelectrons, *Phys. Rev.*, **43**: 727 (1933).
16. Apker, L., E. Taft, and J. Dickey: Energy Distribution of Photoelectrons from Polycrystalline Tungsten, *Phys. Rev.*, **73**: 46 (1948).
17. Berglund, C. N., and W. E. Spicer: Photoemission Studies of Copper and Silver: Theory, *Phys. Rev.*, **136**: A1030 (1964).
18. Berglund, C. N., and W. E. Spicer: Photoemission Studies of Copper and Silver: Experiment, *Phys. Rev.*, **136**: A1044 (1964).
19. Spicer, W. E.: Optical Transitions in Which Crystal Momentum Is Not Conserved, *Phys. Rev. Letters*, **11**: 243 (1963).
20. Fowler, R. H.: Statistical Mechanics, Cambridge University Press, New York and London, 1936.
21. Condon, E. U.: External Photoelectric Effect of Semiconductors, *Phys. Rev.*, **54**: 1089 (1938).
22. Taft, E., and L. Apker: Photoelectric Determination of the Fermi Level at Amorphous Arsenic Surfaces, *Phys. Rev.*, **75**: 1181 (1949).
23. Apker, L., E. Taft, and J. Dickey: Photoelectric Emission and Contact Potentials of Semiconductors, *Phys. Rev.*, **74**: 1462 (1948).
24. Gobelli, G. W., and F. G. Allen: Photoelectric Properties of Cleaved GaAs, GaSb, InAs, and InSb Surfaces; Comparison with Si and Ge, *Phys. Rev.*, **137**: A245 (1965).
25. Kane, E. O.: Theory of Photoelectric Emission from Semiconductors, *Phys. Rev.*, **127**: 131 (1962).
26. Gobelli, G. W., and F. G. Allen: Direct and Indirect Excitation Processes in Photoelectric Emission from Silicon, *Phys. Rev.*, **127**: 141 (1962).
27. Spicer, W. E., and G. J. Lapeyre: Photoemission Investigation of the Band Structure of PbTe, *Phys. Rev.*, **139**: A565 (1965).
28. Brust, D.: Band-theoretic Model for the Photoelectric Effect in Silicon, *Phys. Rev.*, **139**: A489 (1965).
29. Spicer, W. E., and R. E. Simon: Photoemissive Studies of the Band Structure of Silicon, *Phys. Rev. Letters*, **9**: 385 (1962).
30. Allen, F. G., and G. W. Gobelli: Work Function, Photoelectric Threshold, and Surface States of Atomically Clean Silicon, *Phys. Rev.*, **127**: 150 (1962).